

REPORT DOCUMENTATION PAGE

*Form Approved
OMB No. 0704-0188*

The public reporting burden for this collection of information is estimated to average 1 hour per response, including the time for reviewing instructions, searching existing data sources, gathering and maintaining the data needed, and completing and reviewing the collection of information. Send comments regarding this burden estimate or any other aspect of this collection of information, including suggestions for reducing the burden, to the Department of Defense, Executive Services and Communications Directorate (0704-0188). Respondents should be aware that notwithstanding any other provision of law, no person shall be subject to any penalty for failing to comply with a collection of information if it does not display a currently valid OMB control number.

PLEASE DO NOT RETURN YOUR FORM TO THE ABOVE ORGANIZATION.

1. REPORT DATE (DD-MM-YYYY)		2. REPORT TYPE		3. DATES COVERED (From - To)	
4. TITLE AND SUBTITLE				5a. CONTRACT NUMBER	
				5b. GRANT NUMBER	
				5c. PROGRAM ELEMENT NUMBER	
6. AUTHOR(S)				5d. PROJECT NUMBER	
				5e. TASK NUMBER	
				5f. WORK UNIT NUMBER	
7. PERFORMING ORGANIZATION NAME(S) AND ADDRESS(ES)				8. PERFORMING ORGANIZATION REPORT NUMBER	
9. SPONSORING/MONITORING AGENCY NAME(S) AND ADDRESS(ES)				10. SPONSOR/MONITOR'S ACRONYM(S)	
				11. SPONSOR/MONITOR'S REPORT NUMBER(S)	
12. DISTRIBUTION/AVAILABILITY STATEMENT					
13. SUPPLEMENTARY NOTES					
14. ABSTRACT					
15. SUBJECT TERMS					
16. SECURITY CLASSIFICATION OF:			17. LIMITATION OF ABSTRACT	18. NUMBER OF PAGES	19a. NAME OF RESPONSIBLE PERSON
a. REPORT	b. ABSTRACT	c. THIS PAGE			19b. TELEPHONE NUMBER (Include area code)

PUBLICATION OR PRESENTATION RELEASE REQUEST

15-1231-1295

Prokey: 9841

NRLINST 5510.40

1. REFERENCES AND ENCLOSURES	2. TYPE OF PUBLICATION OR PRESENTATION	3. ADMINISTRATIVE INFORMATION
Ref: (a) NRL Instruction 5800.2 (b) NRL Instruction 5510.40E Encl: (1) Two copies of subject publication/presentation URGENT	<input type="checkbox"/> Abstract only, published <input type="checkbox"/> Book author <input type="checkbox"/> Book editor <input checked="" type="checkbox"/> Conference Proceedings (refereed) <input type="checkbox"/> Journal article (refereed) <input type="checkbox"/> Oral Presentation, published <input type="checkbox"/> Video <input type="checkbox"/> Poster <input type="checkbox"/> Abstract only, not published <input type="checkbox"/> Book chapter <input type="checkbox"/> Multimedia report <input type="checkbox"/> Conference Proceedings (not refereed) <input type="checkbox"/> Journal article (not refereed) <input type="checkbox"/> Oral Presentation, not published <input type="checkbox"/> Other, explain	STRN <u>NRL/PP/7330-15-2558</u> Route Sheet No. <u>7330/</u> Job Order No. <u>73-N2D6-05-5</u> Classification U <u> </u> S <u> </u> C <u> </u> FOUO <u> </u> Sponsor <u>NRL Code 1001-Karles</u> Sponsor's approval <u>yes</u> (attached) (*Required if research is other than 6.1/6.2 NRL or ONR unclassified research or if publication/presentation is classified)

ALL DOCUMENTS/PRESENTATIONS MUST BE ATTACHE

4. AUTHOR

Title of Paper or Presentation
 A controlled laboratory environment to study EO signal degradation due to underwater turbulence

AUTHOR(S) LEGAL NAME(S) OF RECORD (First, MI, Last), CODE, (Affiliation if not NRL).
 Silvia Matt 7333, Weilin Hou 7333, Wesley A. Goode 7333, Guigen Liu University of Nebraska-Lincoln, Ming Han University of Nebraska-Lincoln, A. Kanaev NRL Code 5662, S.R. Restaino NRL Code 7210,

This paper will be presented at the SPIE DSS
 (Name of Conference)

20-APR - 24-APR-15, Baltimore, MD, Unclassified
 (Date, Place and Classification of Conference)

and/or for published in SPIE DSS, Unclassified
 (Name and Classification of Publication)

5. CERTIFICATION OR CLASSIFICATION

It is my opinion that the subject paper (is) (is not x) classified, in accordance with reference (b) and this paper does not violate any disclosure of trade secrets or suggestions of outside individuals or concerns which have been communicated to the NRL in confidence.

This subject paper (has) (has never x) been incorporated in an official NRL Report.

Silvia Matt, 7333
 Name and Code (Principal Author) (Legal Name of Record and Signature Only)

Matt
 (Signature)

6. ROUTING/APPROVAL (NOTE: if name other than your legal name of record is mentioned on the publication or presentation itself, add an explanatory note in the "Comments" section below next to your signed legal name of record)

CODE	SIGNATURE	DATE	COMMENTS
Co-Author(s) Silvia Matt, 7333	<i>Matt</i>	4/16/15	Need by <u>20 April 2015</u> This is a Final Security Review. Any changes made in the document, after approved by Code 1231, nullify the Security Review.
Branch Head Richard L. Crout, 7330	<i>Richard Crout</i>	4-16-15	
Division Head Richard Bevilacqua, 7200	<i>Richard Bevilacqua</i>	4/16/15	1. To the best knowledge of this Division, the subject matter of this publication (has <u> </u>) (has never <u>x</u>) been classified.
Ruin H. Preller, 7300	<i>Ruin H. Preller</i>	4-16-15	2. This paper (does <u> </u>) (does not <u>x</u>) contain any military critical technology.
ADOR/Director NCST E. R. Franchi, 7000	<i>Edward R. Franchi</i>	4/17/15	
DOR/CO Security, Code 1231	<i>Shannon Menti</i>	4/20/15	A copy of the paper, abstract or presentation is filed in this office.
Associate Counsel, Code 1008.3			
Public Affairs (Unclassified/Unmiffed Only), Code 7030.4	<i>Shannon Menti</i>	4-27-15	
Division, Code			
Author, Code			

S

A controlled laboratory environment to study EO signal degradation due to underwater turbulence

Silvia Matt^{*a}, Weilin Hou^a, Wesley Goode^a, Guigen Liu^b, Ming Han^b, Andrey Kanaev^c, Sergio Restaino^c

^aNaval Research Laboratory, Stennis Space Center, MS 39426, USA; ^bDepartment of Electrical Engineering, University of Nebraska-Lincoln, Lincoln, NE 68588, USA; ^cNaval Research Laboratory, Washington DC, DC 20375, USA

ABSTRACT

Temperature microstructure in the ocean can lead to localized changes in the index of refraction and can distort underwater electro-optical (EO) signal transmission. A similar phenomenon is well-known from atmospheric optics and generally referred to as “optical turbulence”. Though turbulent fluctuations in the ocean distort EO signal transmission and can impact various underwater applications, from diver visibility to active and passive remote sensing, there have been few studies investigating the subject. To provide a test bed for the study of impacts from turbulent flows on underwater EO signal transmission, and to examine and mitigate turbulence effects, we set up a laboratory turbulence environment allowing the variation of turbulence intensity. Convective turbulence is generated in a large Rayleigh-Bénard tank and the turbulent flow is quantified using high-resolution Acoustic Doppler Velocimeter profilers and fast thermistor probes. The turbulence measurements are complemented by computational fluid dynamics simulations of convective turbulence emulating the tank environment. These numerical simulations supplement the sparse laboratory measurements. The numerical data compared well to the laboratory data and both conformed to the Kolmogorov spectrum of turbulence and the Batchelor spectrum of temperature fluctuations. The controlled turbulence environment can be used to assess optical image degradation in the tank in relation to turbulence intensity, as well as to apply adaptive optics techniques. This innovative approach that combines optical techniques, turbulence measurements and numerical simulations can help understand how to mitigate the effects of turbulence impacts on underwater optical signal transmission, as well as advance optical techniques to probe oceanic processes.

Keywords: Optical turbulence, turbulence measurements, Rayleigh-Bénard tank, numerical simulation, temperature measurements, computational fluid dynamics, oceanic optics

1. INTRODUCTION

“Optical turbulence” is a well-known concept in atmospheric optics where it describes the degradation of EO transmission caused by variations in the index of refraction of air due to turbulence-induced temperature changes along the optical path. This is the same type of phenomenon that occurs when looking at air over a hot road or burning candle. The same concept applies underwater, and here, the visual disturbance can be caused by variations in either temperature or salinity that are associated with turbulent microstructure. Most often, temperature fluctuations are the dominating factor affecting the index of refraction [1], except in the case of strong freshwater or salt water influence, such as in river outflows or estuaries, or possibly in surface lenses generated by rainfall. In this study, we neglect the influence of salinity and instead focus on the effect of temperature.

Underwater “optical turbulence” at sea was investigated in the 1970s by [2], who used this term to describe “small inhomogeneities in the index of refraction of seawater, their origins, and the effects they have on underwater optical systems”. Possibly due to the fact that it is secondary to particle scattering in many locations, the phenomenon of “optical turbulence” in the ocean has since not received widespread attention, even though it can affect a wide range of applications, from diver visibility to active and passive remote sensing. More recently, [1] looked at the effect of “light scattering on oceanic turbulence” with numerical studies compared to measurements in a small laboratory tank. Two recent field studies aimed at characterizing naturally-occurring “optical turbulence” in the aquatic environment highlight the difficulties associated with collecting concurrent data on optics and turbulence in the ocean [3] or lakes [4].

*silvia.matt@nrlssc.navy.mil

Field data are generally affected by a number of external parameters, including platform motion polluting the velocity data and scattering due to particles degrading the optical signal, and to reduce the number of parameters involved, we developed a laboratory environment for the study of underwater “optical turbulence”. The laboratory setup permits the variation of turbulence intensity and thus a “controlled turbulence environment” is generated, which also provides a framework for repeatable experiments. The laboratory experiments are supplemented by numerical simulations using computational fluid dynamics (CFD). The numerical simulations provide full fields of temperature and velocity and thus provide a better view of the large-scale flow field and distribution of turbulence parameters than could be gathered with the sparse laboratory measurements alone.

To quantify the impact of turbulent fluctuations on optical signal transmission, the optical turbulence parameter S_n can be calculated. S_n is the oceanic equivalent of the atmospheric optical turbulence coefficient C_n^2 and is a function of turbulent kinetic energy and temperature variance dissipation rates, ϵ and χ , respectively [5][6]:

$$S_n \sim \chi \epsilon^{-1/3} \quad (1)$$

Thus, in order to estimate S_n and the amount of image degradation from turbulence, we need information on both velocity and temperature fluctuations. These measurements need to be of sufficient resolution to allow inferring dissipation rates ϵ and χ .



Figure 1. Laboratory tank at NRLSSC. The photo on the right shows the Vectrino profiler ADV and the CT temperature probe.

2. METHODS

Laboratory Setup

The laboratory setup consists of a large acrylic tank which is 5m long and has a cross section of 0.5m by 0.5m and is outfitted with stainless steel plates at the bottom and top that can be temperature controlled (Fig. 1, left). In this tank, convective Rayleigh-Bénard type turbulence is generated by heating and cooling the bottom and top, respectively. The strength of the convective turbulence in the tank is a function of the temperature difference across the tank and can be characterized in terms of the Rayleigh number, defined as

$$Ra = g\alpha\Delta Td^3/(\nu D_T) \quad (2)$$

Where g is the acceleration due to gravity, α is the thermal expansion coefficient, ΔT is the temperature difference between the plates, d is the distance between the plates, ν is the kinematic viscosity, and D_T is the thermal diffusivity.

The Rayleigh number of the flow can be changed by changing the plate temperatures, and thus the turbulence intensity can be varied. In our experiments, Ra ranges from $1.5 \cdot 10^{10}$ to around $4 \cdot 10^{10}$, corresponding to a temperature difference ΔT between the plates of 6K and 16K, respectively.

The turbulence in the tank is quantified by high-resolution Acoustic Doppler Velocimeter profilers (Nortek Vectrino Profiler) and fast thermistor probes (PME high-resolution conductivity-temperature (CT) probe) (Fig. 1, right). These instruments provide high-resolution velocity and temperature measurements, at 100 and 64Hz, respectively. Three ADVs and two CT probes were mounted in the tank and collected time series of high-resolution velocity and temperature/conductivity for the subsequent estimation of ε and χ . Data were collected at a sampling frequency of 100Hz with the Vectrino Profiler and at 64Hz with the CT probes, which were controlled by a Nortek Vector ADV in our setup. Turbulent kinetic energy dissipation rate ε and temperature variance dissipation rate χ were calculated from the velocity and temperature measurements via spectral fitting to Kolmogorov spectra (for velocity) and Batchelor spectra (for temperature) and compared to values obtained from the numerical simulations of convective turbulence in the tank for comparable Rayleigh number and setup [7][8][9][10]. The turbulence data is put into the context of measurements of optical target clarity, by placing a high-speed imaging camera and active optical target, an iPad displaying optical resolution charts, at opposite ends of the tank, providing an optical path length of around 5m. To quantify the extent of image degradation from optical turbulence, an image quality metric, namely the Structural Similarity Index Method (SSIM) can be applied [11]. The SSIM measures the similarity between two images, where one is considered to be of “perfect quality”.

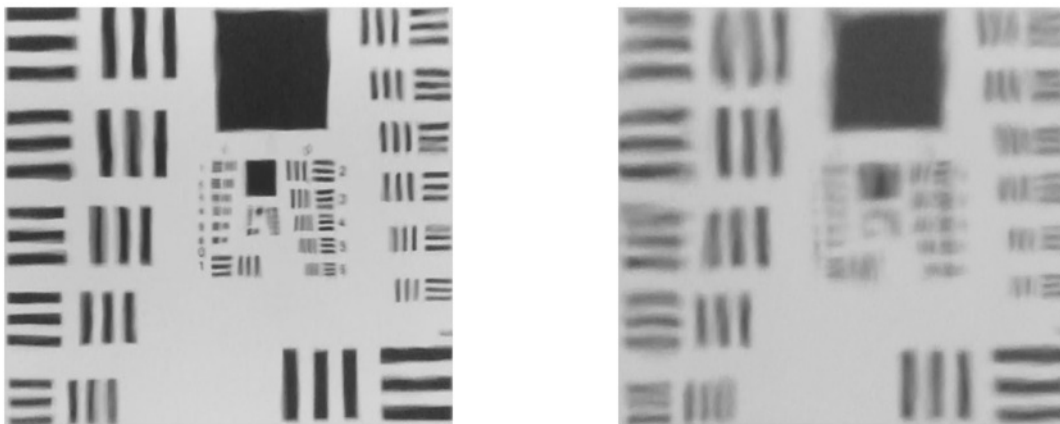


Figure 2. Image degradation for different “optical turbulence” strengths. The images are taken with an optical path of 5m (the length of the laboratory tank) of an optical resolution chart across a region of turbulent water. Left is for a lower yet still “strong” level of optical turbulence and on the right is the highest level of turbulence (“extreme”) we can achieve in the tank.

Images from the laboratory show the image degradation due to optical turbulence for a case of “strong” (Fig. 2, left, $\Delta T \approx 6K$) and “extreme” optical turbulence (Fig. 2, right, $\Delta T \approx 16K$). Here, particle scattering is secondary to the changes in the index of refraction due to temperature microstructure. Note that the effect of optical turbulence is more pronounced at the higher spatial frequencies. When applying the SSIM metric to a sequence of video images in order to quantify the extent of image degradation from optical turbulence, the differing amounts of image degradation for the two turbulence cases is confirmed [12].

Numerical Tank

The sparse laboratory measurements (three Vectrino Profilers and two temperature probes) were complemented by CFD simulations of the convective tank. These three-dimensional, very high-resolution, non-hydrostatic numerical simulations provide full fields of temperature and velocity for the estimation of turbulence parameters and their impact on the optics.

The numerical experiments were performed with the open-source CFD package OpenFOAM using a Large-Eddy Simulation (LES) approach. In LES, the larger-scale eddies in the flow are explicitly resolved, while the scales smaller than the grid-size are modeled [13]. The traditional Smagorinsky model was chosen as the sub-grid scale model [14]. Here, we present results from a very high-resolution, millimeter-scale simulation with $\Delta x = \Delta y = 5mm$, $\Delta z = 2.5mm$, which corresponds to 20 million grid points in the 5m by 0.5m by 0.5m domain (Fig. 3). Exploratory simulations at lower resolution ($\Delta x = \Delta y = \Delta z = 1cm$) were run on a modern, high-performance, dual six-core Linux desktop, whereas

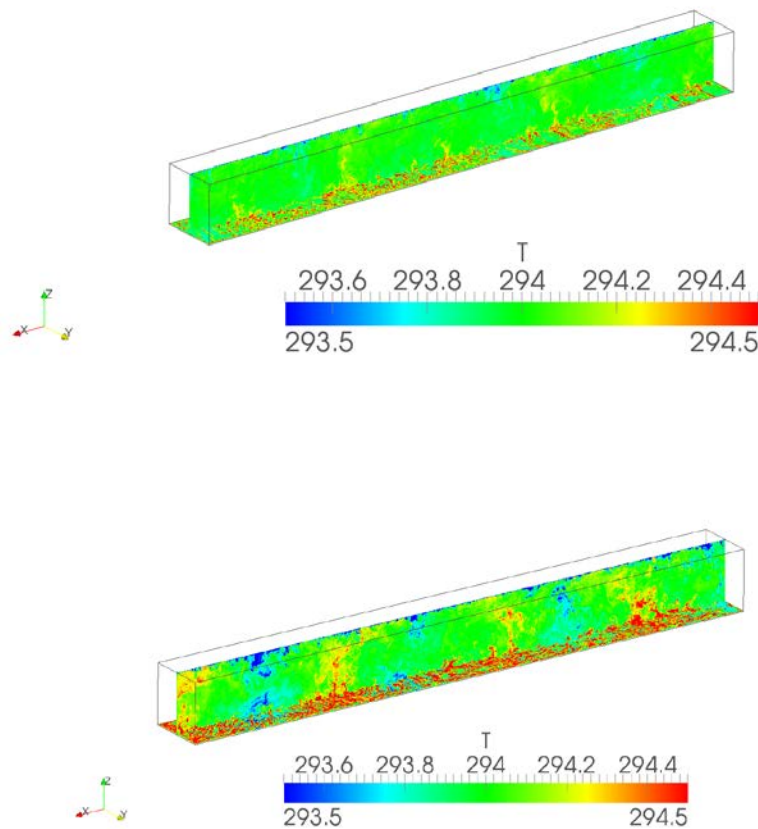


Figure 3. “Numerical Tank” used to simulate Rayleigh-Bénard convection and emulating the laboratory tank setup. The temperature field (in K) is shown and several convective plumes are visible. Top is “strong” optical turbulence, bottom is for “extreme” optical turbulence. (Note that this figure appears in color in the web version of this article.)

production runs at the millimeter-scale resolution required High-Performance Computing resources at the DoD Supercomputing Resource Center, due to the high computational cost.

Temperature and velocity from the numerical simulations provide a view of the overall circulation in the tank, thus supplementing the sparse laboratory measurements. The simulations illustrate that convective cells are established in the tank and a more detailed description of the fields in the tank has been reported in [12]. The size and number of the convective cells that develop in the tank are a function of the tank dimensions, in particular the tank height, since the water rises and sinks and gets diverted once it reaches the solid boundaries at the top and bottom. With a tank of depth $d = 0.5\text{m}$ and length $L = 5\text{m}$, we observe on the order of ten convective cells in our domain. In addition to the convective cells, secondary circulations, namely in the cross-sectional direction, develop in the domain. These circulations can be visually confirmed in the laboratory when adding a tracer to the fully developed flow field, such as, for example, the seeding material needed to collect ADV data. The model temperature fields allow the calculation of the index of refraction (IOR) from these fields, using the empirical relation described in [15]. These fields, which have been reported in [12], can then provide an illustration of the disturbance expected to be encountered by an optical beam passing through the tank.

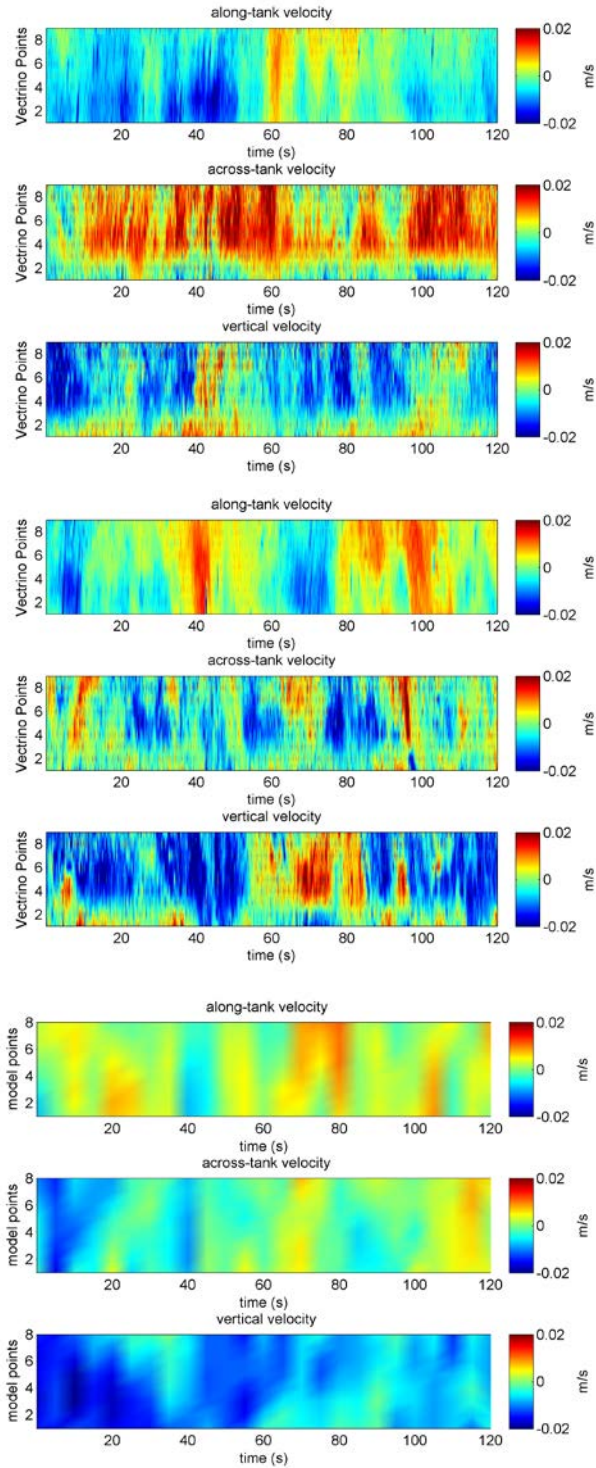


Figure 4. Vectrino Profiler data from laboratory tank for “strong” (top) and “extreme” (middle) optical turbulence. Results from the numerical simulation of the tank are shown at the bottom, for the case of “extreme” turbulence. (Note that this figure appears in color in the web version of this article.)

3. RESULTS

Comparing data from the Vectrino Profiler for “strong” and “extreme” optical turbulence, shows the maximum velocities are on the order of 2 cm/s for both cases (Fig. 4). The Vectrino data is shown for all nine points from the Vectrino Profiler, which cover a horizontal sampling volume of $\sim 3\text{cm}$. Comparing the laboratory data to output from the numerical model from a similar location in the tank, reveals that the variability time scales and velocity magnitudes are similar. Note that the Vectrino data is collected at a sampling frequency of 100 Hz, whereas the model data is subsampled every 5s, due to the large amount of data generated. The model time step is $\Delta t = 0.01\text{s}$, so it is possible to save model data at 100 Hz for a more direct comparison with the Vectrino data.

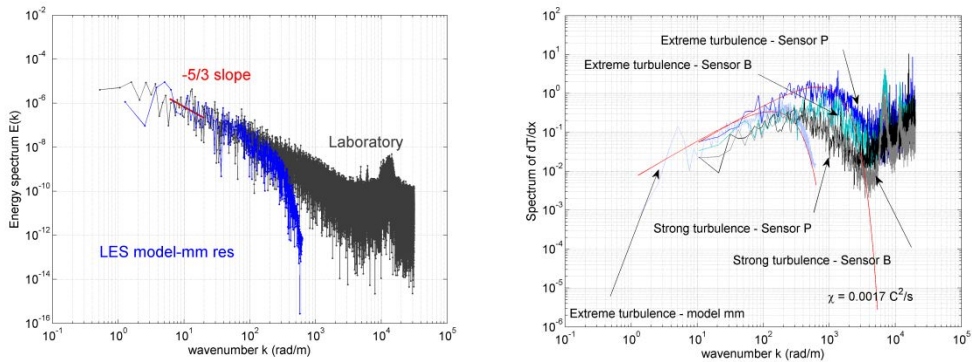


Figure 5. Energy spectra (left) and temperature gradient spectra (right) from laboratory and model data. The energy spectra show no significant change for different convective turbulence strengths [12] and are shown here only for the highest level of turbulence. The temperature gradient spectra do resolve the difference in turbulence strengths. (Note that this figure appears in color in the web version of this article.)

To further quantify the turbulence in the tank and to estimate the turbulence parameters necessary to estimate the optical turbulence coefficient S_n , we calculate turbulent kinetic energy dissipation rates ϵ and temperature variance dissipation rates χ from the data collected in the laboratory. These values are then compared to ϵ and χ calculated from the numerical experiments. The numerical data compared well to the laboratory data and both conformed to the Kolmogorov spectrum of turbulence and the Batchelor spectrum of temperature gradients (Fig. 5). The numerical model was able to qualitatively reproduce the turbulence fields observed in the laboratory tank. Quantitatively, the numerical simulations are consistent with the observed ϵ in the tank, despite the fact that they do not resolve the spectrum down to the Kolmogorov microscale, which is on the order of mm for this flow. The laboratory data show that even for convective strength with dramatically different impact on the optics (see Fig. 2), the ϵ in the tank remains within one order of magnitude. To illustrate how ϵ is expected to vary across the tank cross-section, we can take the spectrum from the numerical model data at every 5m-long velocity section in the tank, for each x- and z-position (Fig. 6).

The value of ϵ stays mostly within one order of magnitude across the tank. The variation near the boundaries due to boundary layer effects can be expected, and is consistent with the cross-sectional circulation seen in the velocity field. While the ϵ from the model is consistent with the laboratory value, both are of $O(10^{-7} \text{ W/kg})$ for the experiments shown, the numerical simulations do not fully resolve the temperature gradients and thus underestimate χ , even at the high resolution used in our experiments ($\Delta x = \Delta y = 5\text{mm}$, $\Delta z = 2.5\text{mm}$; 20 M grid points). The values of χ from both the laboratory and the numerical simulations show a significant difference for different convective turbulence strengths, but since the estimates from the numerical simulations are strongly resolution dependent and lower than the laboratory values for comparable turbulence strength, estimating the model sub-grid scale contribution to χ is of critical importance and is the subject of ongoing work. Since the effect on the optics is driven by changes in the index of refraction due to temperature variations, these results reemphasize the importance of characterizing in detail the temperature distribution to assess the impact of the turbulent fluctuations on the optics.

The PME microstructure temperature sensor (GE FP07 thermistor) has been reported to resolve the variance in the temperature gradient spectrum up to a frequency of about 25Hz [10]. A single-pole response function can be applied to help with the sensor related roll-off at higher frequencies or wavenumbers. Additionally, noise in the measurements may make it impossible to resolve the spectrum to the Batchelor number cut-off. In order to address this need for improved higher-resolution temperature measurements, we tested a novel miniature fiber-optic sensor for high-resolution and high-

speed temperature. A detailed description of this sensor can be found in a companion paper by Liu et al. [16]. Figure 7 shows three channels of this new fiber-optic sensor mounted next to the PME microstructure temperature sensor in the tank.

The new high-resolution sensor collected temperature data at 500Hz, revealing high-resolution details in temperature variation (Fig. 8). The sensor was able to resolve the temperature gradient spectrum beyond the Batchelor number cut-off; a noted improvement over the FP07 thermistor (Fig. 9).

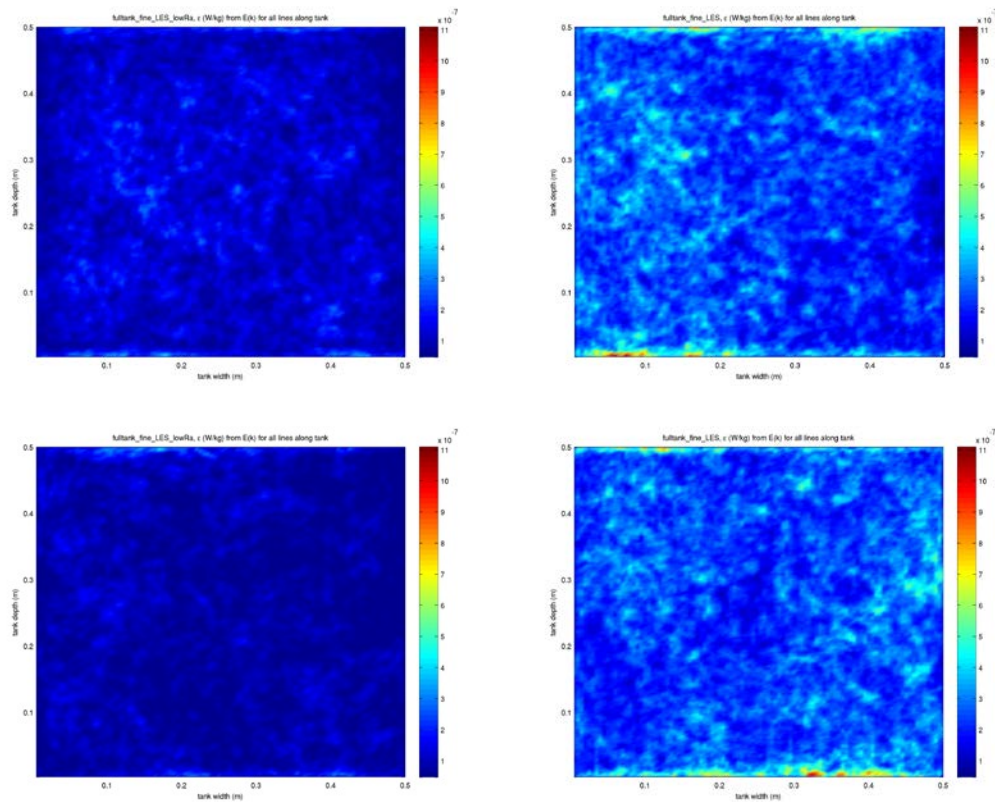


Figure 6. Turbulent kinetic energy dissipation rate ϵ from velocity section along the length of the tank at each x-z-point, in W/kg. Left row: low Ra turbulence at times $t = 250$ s (top) and $t = 1675$ s (bottom). Right row: high Ra turbulence at times $t = 250$ s (top) and $t = 1675$ s (bottom). (Note that this figure appears in color in the web version of this article.)



Figure 7. Fiber optics sensors next to PME microstructure temperature sensor (FP07) in the tank.

4. CONCLUSIONS

In order to study the impact of temperature microstructure on underwater optical signal transmission, we performed experiments in a controlled laboratory environment complemented by high-resolution, non-hydrostatic numerical simulations. The goal was to develop a setup where turbulence levels can be controlled and fully characterized. This setup, which allows for repeatable experiments under controlled conditions, can help us understand processes involved in optical turbulence and provides a platform for the testing of optical techniques to mitigate turbulence effects underwater, such as the use of adaptive optics techniques to mitigate underwater optical turbulence [17][18].

Optical turbulence is mainly due to temperature (or salinity) variations affecting the IOR of water, and to adequately describe the effect on the optics, it is particularly critical to resolve the temperature gradients. This can present a challenge in both the laboratory and the model, due to noise and resolution requirements, respectively. In the model, further work is needed to address questions related to sub-grid scale contributions in LES to the rate of temperature variance dissipation. In the laboratory, the unique asset of the Rayleigh-Bénard convective tank allowed us to test a novel miniature fiber-optic sensor for high-resolution and high-speed temperature to address the need for improved temperature measurements. The new high-resolution sensor collected temperature data at 500Hz and resolved the temperature gradient spectrum beyond the Batchelor number cut-off; a noted improvement over the FP07 sensor, which is generally described as resolving the variance in the spectrum up to a frequency of about 25Hz.

Our unique approach of integrating optical techniques, turbulence measurements and numerical simulations can help advance our understanding of how to mitigate the effects of turbulence impacts on underwater optical signal transmission, as well as on the use of optical techniques to probe oceanic processes.

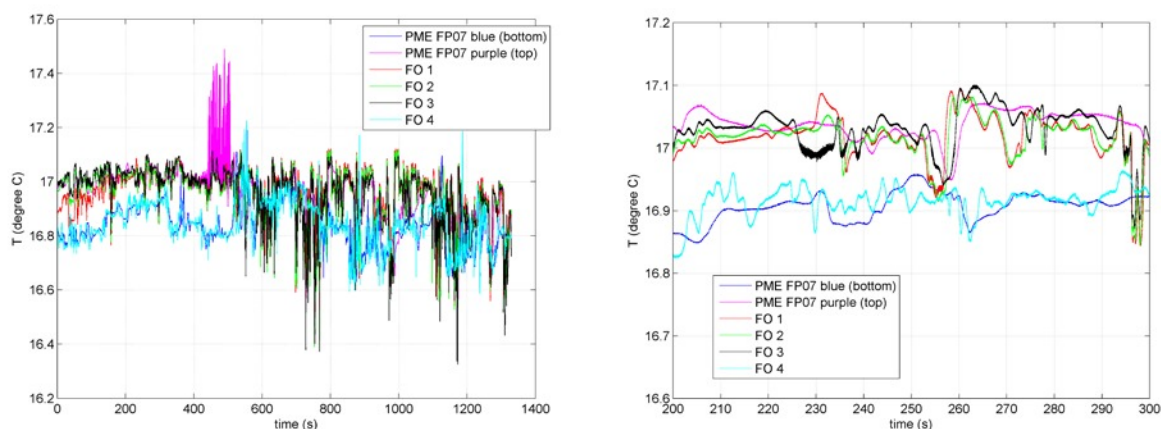


Figure 8. Temperature time series FP07 compared with FOTS fiber optics sensor. Left: time series over approximately 20 minutes, right: close-up of time = 200s to 300s, showing the detail in the data from FOTS. (Note that this figure appears in color in the web version of this article.)

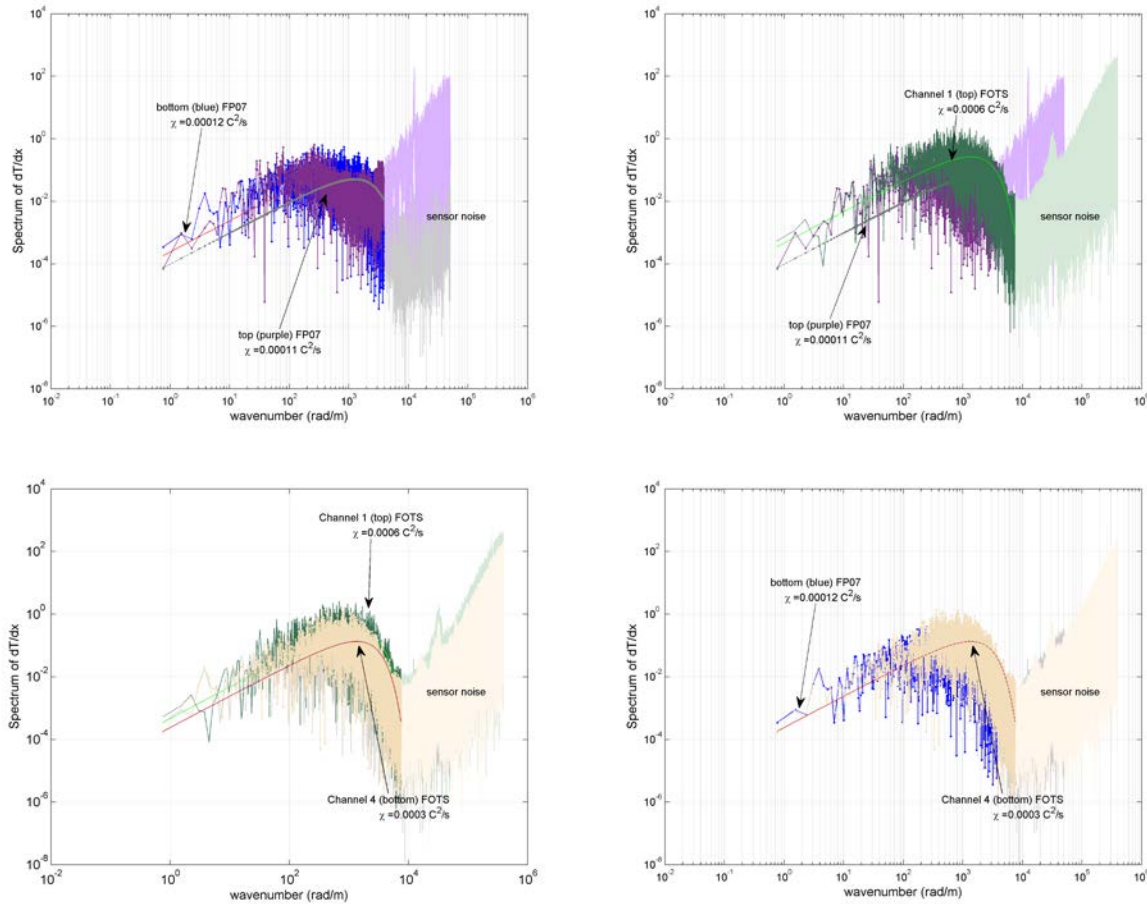


Figure 9. Temperature gradient spectrum of data from FP07 compared with FOTS, showing that FOTS appears to resolve the spectrum to the Batchelor cut-off wavenumber. (Note that this figure appears in color in the web version of this article.)

ACKNOWLEDGMENTS

We thank Danielle Wain, Cynthia Bluteau and Barry Ruddick for sharing their data processing routines. Sarah Woods contributed to the tank design and early instrumental setup. We are grateful to Joe Calantoni for allowing us the use of his Vectrino II instrument. This project was supported by ONR/NRL 73-4951/73-6604. Silvia Matt was supported by a National Research Council (NRC) Research Associateship and a NRL Karle Fellowship.

REFERENCES

- [1] D. Bogucki, J. Domaradzki, R. Ecke, and C. Truman, "Light scattering on oceanic turbulence," *Appl. Opt.*, 43, pp. 5662-5668, 2004.
- [2] G. D. Gilbert, and R. C. Honey, "Optical turbulence in the sea," *Proc. SPIE 0024, Underwater Photo-Optical Instrumentation Applications III*, 49, 1971.
- [3] S. Matt, W. Hou, S. Woods, W. Goode, E. Jarosz, and A. Weidemann, "A Novel Platform to Study the Effect of Small-Scale Turbulent Density Fluctuations on Underwater Imaging in the Ocean," *Methods in Oceanography*, 11, pp. 39–58, 2014.
- [4] W. Hou, S. Woods, E. Jarosz, W. Goode, and A. Weidemann, "Optical turbulence on underwater image degradation in natural environments," *Appl. Opt.*, 51, pp. 2678– 2686, 2012.

- [5] W. Hou, "A simple underwater imaging model," *Opt. Lett.*, 34, pp. 2688-90, 2009.
- [6] M. C. Roggemann, and B. M. Welsh, [Imaging through Turbulence], CRC Press, Boca Raton, Florida, USA, 1996.
- [7] H. Tennekes and J. L. Lumley, [A first course in turbulence], MIT Press, 1972.
- [8] P. Rusello and E. Cowen, "Turbulent dissipation estimates from pulse coherent doppler instruments," *Current, Waves and Turbulence Measurements (CWTM)*, 2011 IEEE/OES 10th, pp. 167–172, 2011.
- [9] B. Ruddick, A. Anis, and K. Thompson, "Maximum likelihood spectral fitting: The Batchelor spectrum," *J. Atmos. Oceanic Technol.*, 17, pp. 1541–1555, 2000.
- [10] J. Moum and J. Nash, "Mixing measurements on an equatorial ocean mooring," *J. Atmos. Oceanic Technol.*, 26, pp. 317–336, 2009.
- [11] Z. Wang, A. C. Bovik, H. R. Sheikh, and E. P. Simoncelli, "Image quality assessment: From error visibility to structural similarity," *IEEE Transactions on Image Processing*, 13, pp. 600–612, 2004.
- [12] Matt, S., W. Hou, and W. Goode, "The Impact of Turbulent Fluctuations on Light Propagation in a Controlled Environment," *Proc. SPIE 9111*, 911113, 2014.
- [13] P. Sagaut, [Large Eddy Simulation for Incompressible Flows], Springer, 1998.
- [14] Smagorinsky, J., "General Circulation Experiments with the Primitive Equations. I. The Basic Experiment," *Month. Wea. Rev.*, 91, 99–164, 1963.
- [15] X. Quan and E. S. Fry, "Empirical equation for the index of refraction of seawater," *Applied Opt.*, 34, pp. 3477–3480, 1995.
- [16] Liu, G., M. Han, W. Hou, S. Matt, W. Goode: A miniature fiber-optic sensor for high-resolution and high-speed temperature sensing in ocean environment, *SPIE 9459*, (2015), *Proceedings SPIE DSS*, 2015.
- [17] Restaino, S. R., W. Hou, A. Kanaev, S. Matt, and C. Font: Adaptive optics correction of a laser beam propagating underwater, *Proc. SPIE 9083*, *Micro- and Nanotechnology Sensors, Systems, and Applications VI*, 90830R, 2014.
- [18] Kanaev, A., W. Hou, S. Restaino, S. Matt: Correction methods for underwater turbulence degraded imaging, *Proc. SPIE 9242*, *Optics in Atmospheric Propagation and Adaptive Systems*, 2014.